



# Exploring Nanocrystalline Europium Titanium Niobate as a Dielectric Resonator

Fergy John<sup>a\*</sup>

<sup>a</sup>Department of Physics, St Gregorios College, Kottarakara Kerala 691 531 India

Received 3 June 2021; accepted 13 July 2021

High dielectric constant and low loss nanocrystalline  $\text{EuTiNbO}_6$  ceramic was synthesized through a combustion technique. Phase purity, structure and particle size were examined using X-Ray diffraction, Fourier Transform Raman, Infrared spectroscopy and transmission electron microscopic techniques. The X-Ray diffraction study reveals that the sample crystallizes in orthorhombic aeschynite structure without any impurity. The non-agglomerated particles with narrow particle size distribution were observed in the transmission electron micro graph and the average particle size was found to be 25 nm. The sample attained the 98 % of theoretical density when it was sintered at 1150 °C. The scanning electron micrograph of the sample exhibits non uniform distribution of grains nearly in spherical shape throughout the surface. The Energy dispersive spectrum analysis confirms that the constituent elements are nearly the same atomic percentage as per the chemical formula of the sample. The dielectric properties of the sintered sample were measured in the radio frequency and micro frequency region. The dielectric constant and quality factor of the sample at room temperature are 35 and 23370, respectively. The dielectric studies revealed that the nanocrystalline  $\text{EuTiNbO}_6$  Ceramic is a promising material for dielectric resonator applications.

**Keywords:** Orthorhombic aeschynite structure; Dielectric resonator; Nanocrystalline ceramic; Combustion technique; Dielectric properties

## 1 Introduction

Dielectric resonators are the essential component of the microwave communication systems. The selectivity of the signal and the compactness of the circuit depend up on the high dielectric constant and low dielectric loss of the ceramic used in the resonator circuit. Several microwave dielectric materials have been investigated by the researches for the resonator applications. But in the present context, the drastic development of microwave mobile telecommunication system has forced the need to identify nanostructured dielectric materials with enhanced properties. The properties of RE-Ti-Nb-O<sub>6</sub> using hydrothermal method were first reported by Komkov *et al.*<sup>1</sup>. The dielectric properties in the microwave frequency region of bulk RE-Ti-Nb-O<sub>6</sub> (RE=Ce, Pr, Nd, Sm, Eu, Gd, Tb, Y and Yb) ceramics prepared through the solid state ceramic route were reported by Sebastian *et al.*<sup>2</sup>. The sintering temperature of micro sized Nd-Ti-Nb-O<sub>6</sub> was reduced by the substitution of ZnO<sup>3</sup>. Jacob *et al.* have reported the photoluminescence studies of certain polycrystalline lanthanide titanium tantalates<sup>4</sup>. The improved microwave dielectric properties of yttrium

substituted NdTiTaO<sub>6</sub> ceramics were studied<sup>5</sup>. The nano crystalline RETiNbO<sub>6</sub> (RE = Ce, Pr, Nd and Sm) having low dielectric loss and high dielectric constant was developed by John *et al.*<sup>6</sup>. The variation of the dielectric constant, conductance and loss factor of RETiNbO<sub>6</sub> (RE = Dy, Er, Gd, Yb) with radio frequency range were investigated<sup>7</sup>. The dielectric properties of the samples, Ln<sub>0.8</sub>Lu<sub>0.2</sub>TiNbO<sub>6</sub> (Ln = Ce, Pr, Nd & Sm) in the radio as well as microwave frequencies were investigated<sup>8</sup>. The present study is aimed at exploring the dielectric properties of nano-sized  $\text{EuTiNbO}_6$  in radio as well as microwave frequency ranges. The sample was synthesized by the combustion method and its sintering behavior and microstructure were also investigated.

## 2 Experimental

Nanocrystalline  $\text{EuTiNbO}_6$  (EuTN) was prepared by combustion technique. The reagents used for the preparation of EuTN were, high-purity niobium pentachloride, titanium isopropoxide and Europium oxide. Urea and Citric acid were used as fuel and complexing agent, respectively. Stoichiometric amount of the reagents were dissolved in double distilled water and the oxidant to fuel ratio of the system was adjusted by using concentrated HNO<sub>3</sub> and liquor ammonia<sup>9-11</sup>. The solution containing the

\*Corresponding author: (E-mail: fergypd@gmail.com)

reagents ions was heated using a hot plate at 250 °C in a combustion chamber. On continuous heating, the solution ignited by itself due to self-propagating combustion and voluminous nanopowder was obtained.

### 3 Characterizations

The X-ray diffraction technique (Model: Philips PW1710 diffractometer) was used to determine the structure of the as prepared sample. The Fourier Transform Infrared spectrum of the sample was recorded with a Thermo-Nicolet Avatar 370 Fourier Transform Infrared Spectrometer using the KBr pellet method. The Fourier Transform-Raman spectrum of the sample was recorded at room temperature using a Bruker RFS/100S Spectrometer. Nanoparticle properties such as particle size and morphology of the as prepared sample were examined using transmission electron microscope (Hitachi H-600 Japan). The surface morphology of the sintered sample and the energy dispersive X-ray analysis (EDS) were studied using scanning electron microscopy (JEOL 6390 LV). The dielectric constant ( $\epsilon_r$ ) and the unloaded quality factor ( $Q_u$ ) at microwave frequency range were calculated using the computer interfaced network analyzer Agilent 8753 ET. At radio frequencies, the dielectric parameters such as dielectric constant, conductance and dielectric loss were also measured using an impedance analyzer (HIOKI LCR HI Tester, Model: 3532).

### 4 Results and discussion

The powder XRD pattern of as prepared EuTN is shown in Fig. 1. All the prominent peaks agree well with the standard data (ICDD files 15-0864) and the sample exhibits orthorhombic aeschynite structure

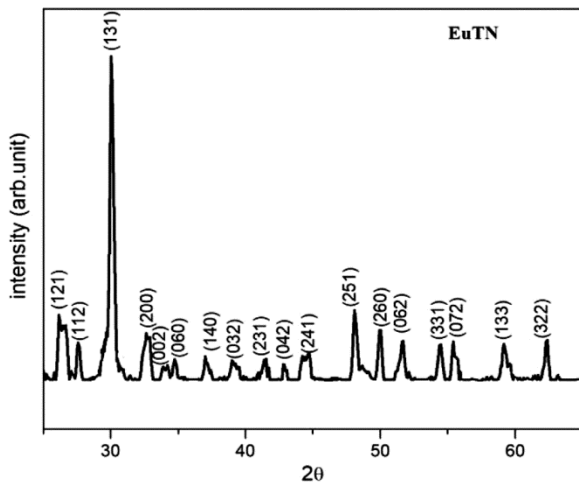


Fig. 1 — The XRD pattern of as-synthesized sample EuTN

with space group Pnma. The diffraction peaks were broad as compared to the bulk  $\text{RETiNbO}_6$  ceramics, which indicate the presence of particles of very small crystallite size<sup>2</sup>. The crystallite size calculated from full-width-half-maximum (FWHM) using Scherrer formula was found to be 22 nm. The structural analysis using XRD data indicate that nanocrystalline EuTN having highest degree of phase purity, was formed during single step the combustion process. It is important to note that the combustion method for the preparation of nanomaterials need not require any calcination as in the case of conventional solid state route. The crystallinity and the formation of single phase nano EuTN through the combustion process itself is confirmed by analyzing the XRD data.

FT Raman spectrum of the EuTN sample recorded at room temperature is presented in Fig. 2. A three dimensional network of corner and edge sharing  $\text{NbO}_6$  octahedra constitute aeschynite orthorhombic structure with the fifteen vibrational degrees of freedom<sup>12</sup>. The six fundamental vibrations of  $\text{NbO}_6$  octahedron with  $O_h$  symmetry represented as,  $\Gamma = A_{1g}(\text{R}) + E_g(\text{R}) + 2F_{1u}(\text{IR}) + F_{2g}(\text{R}) + F_{2u}(\text{Silent})$ . The Raman active  $\nu_1 A_{1g}$ ,  $\nu_2 E_g$ ,  $\nu_3 F_{1u}$ ,  $\nu_4 F_{1u}$ ,  $\nu_5 F_{2g}$  and  $\nu_6 F_{2g}$  modes, give rise to the symmetric and asymmetric stretching and bending vibrations of O–Nb bonds. The  $\nu_1 A_{1g}$ ,  $\nu_2 E_g$  and  $\nu_3 F_{1u}$  modes of  $\text{NbO}_6$  octahedra were obtained at the wave numbers 862, 668 and 452  $\text{cm}^{-1}$ . The IR active asymmetric bending mode  $\nu_4 F_{1u}$  of the sample was active at 410  $\text{cm}^{-1}$ . A very weak intense band at 310  $\text{cm}^{-1}$  is due to symmetric bending  $\nu_5 F_{2g}$  mode of vibration. The inactive  $\nu_6 F_{1u}$  modes were observed as a medium intense band at 257  $\text{cm}^{-1}$  sample. The bands below 200  $\text{cm}^{-1}$  are due to lattice vibrations including

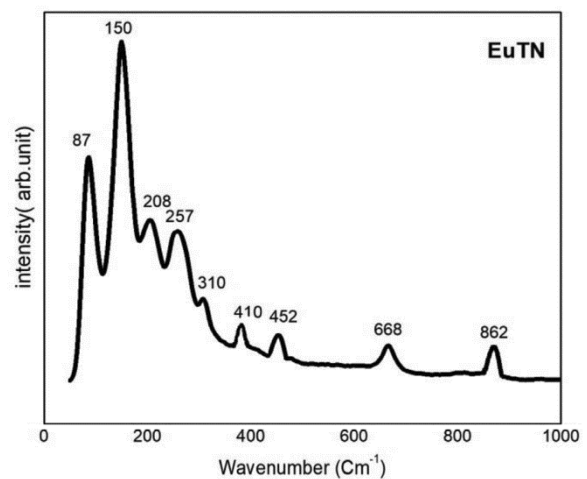


Fig. 2 — The FT Raman spectrum of EuTN

octahedral translation. The slight distortion in the  $\text{NbO}_6$  octahedron in the sample gives rise to the broadening and splitting of the bands. The highly intense band at  $671\text{ cm}^{-1}$  in the FT-IR spectrum shown in Fig. 3 is due to IR active  $\nu_3\text{F}_{1u}$  asymmetric stretching mode of  $\text{NbO}_6$  octahedra. The band due to the bending and stretching vibrations of O-H bond was observed at  $1635\text{ cm}^{-1}$ . The reported modes of vibration for the orthorhombic structure are comparable with the experimental modes of vibrations, thus the existence of orthorhombic structure is confirmed with FT IR and FT Raman studies.

The TEM analysis provides the information about the particle size and morphology of as synthesized nanopowder. Figure 4 shows the TEM image of EuTN, which confirms the narrow particle size distribution and polycrystalline nature of the sample<sup>13</sup>. The particles of as prepared sample are nearly in spherical in shape with homogeneous morphology. The average particle size of non-agglomerated and

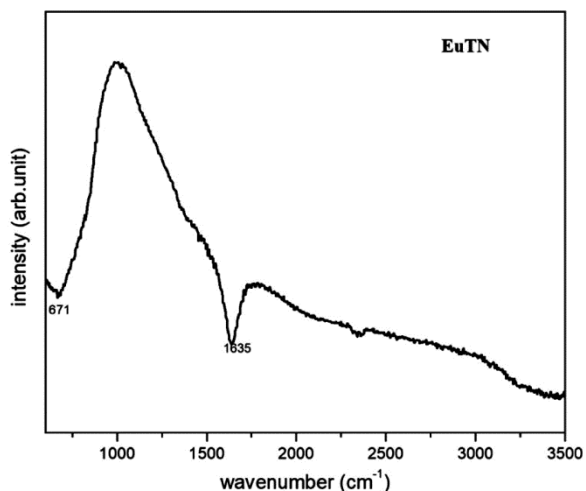


Fig. 3 — The FT-IR spectrum of the as-synthesized sample EuTN

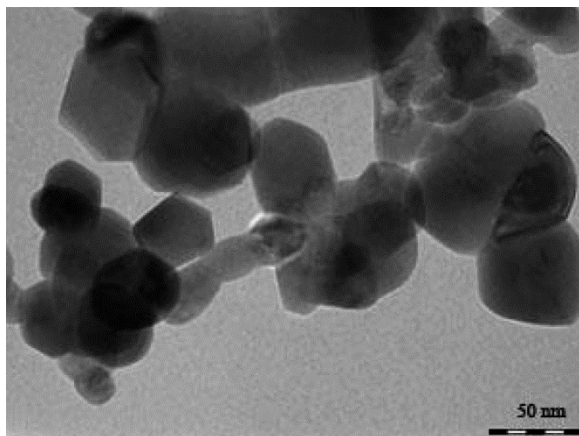


Fig. 4 — The TEM image of as-synthesized powder EuTN

well-defined particles of EuTN calculated from the histogram (shown in Fig. 5) was obtained as 25 nm. The good nanocrystalline nature of the sample EuTN is confirmed from the TEM studies. The sample obtained after the combustion process is crystalline in nature and the all particles are separated by well-defined sharp boundaries without any agglomeration. Hence, the combustion method play a vital role in producing the phase pure, nano sized EuTN particles in a single step synthesis process.

Highly dense pellet form of the powder sample is significant for the dielectric measurements. The sintering characteristic of the nanocrystalline EuTN prepared by combustion method was analyzed systematically. At temperature  $1150\text{ }^\circ\text{C}$ , the sample was well sintered to highly dense form without any structural distortion. In addition, it is observed that the high surface area and surface energy of nano sample leads to good sintering. But, the bulk  $\text{RETiNbO}_6$  samples prepared by conventional solid state ceramic route were sintered at a temperature in the range  $1360\text{--}1400\text{ }^\circ\text{C}$ . Relatively low sintering temperature, fast densification, end product with small grain size and rejection of sintering aids, are the main advantages in the sintering process of the sample prepared exclusively by combustion method. The dielectric properties of a sintered sample mainly depend on the microstructure developed during sintering.

The scanning electron micrograph of EuTN given in Fig. 6 shows the surface morphology of the sintered sample. SEM image exhibits non uniform distribution of grains nearly in spherical shape throughout the surface of the sample. It also shows that the nanocrystalline EuTN sample has achieved

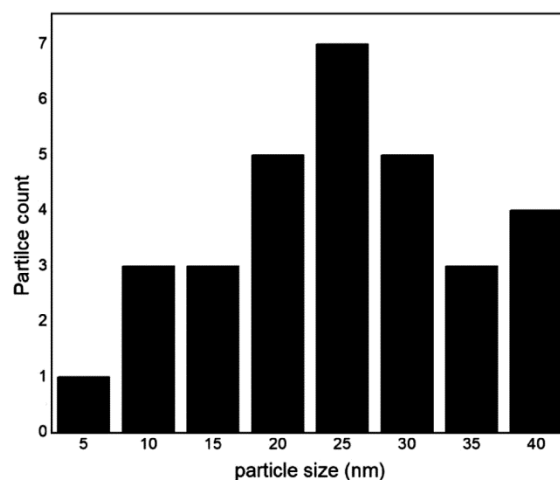


Fig. 5 — Particle size distribution histogram of EuTN

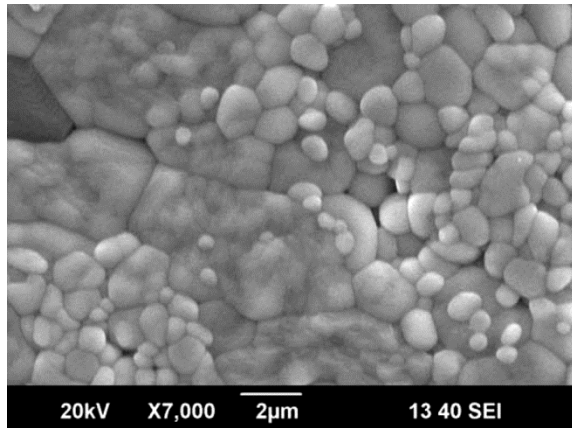


Fig. 6 — The SEM micrograph of EuTN

high densification with negligible porosity due to its high surface area. Grain boundaries play an important role in the preparation of ceramics for dielectric resonators. The grain size of the sample has increased due to the grain boundary merging in the sintering process. The average grain size obtained for the nanocrystalline EuTN after the sintering process is about  $\sim 1\mu\text{m}$ .

The constituent elements of the sample distinguished from the EDS spectrum is shown in Fig. 7. The various Peaks in the spectrum appeared at different values of binding energies correspond to the constituent elements in the sample EuTN. This study demonstrates the presence of stoichiometric concentration of the respective constituents Eu, Nb, Ti, and O, in the sample. EDS spectrum also substantiate the absence of any impurity elements in the as prepared sample.

The materials with high dielectric constant and low dielectric loss are used as microwave dielectric resonators in communication systems. The microwave dielectric properties such as dielectric constant and quality factor of the system EuTN were investigated and estimated as 35 and 23370, respectively. Sebastian *et al.* have reported the dielectric constant and quality factor of pure micro crystalline  $\text{LnTiNbO}_6$  in microwave frequency range prepared by conventional solid state ceramic method. The sample has very high-quality factor than the earlier reports due to the space charge polarization and Nano size of the particles<sup>2</sup>.

The variations of dielectric constant, loss factor ( $\tan \delta$ ) and conductance with logarithm of frequency at room temperature were studied in the radio frequency domain. Due to the mobility of charge carriers in dielectric material, the value of dielectric

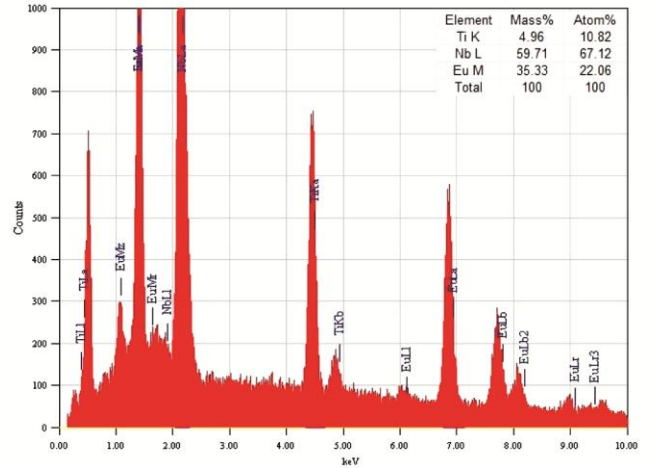


Fig. 7 — The EDS spectrum of EuTN

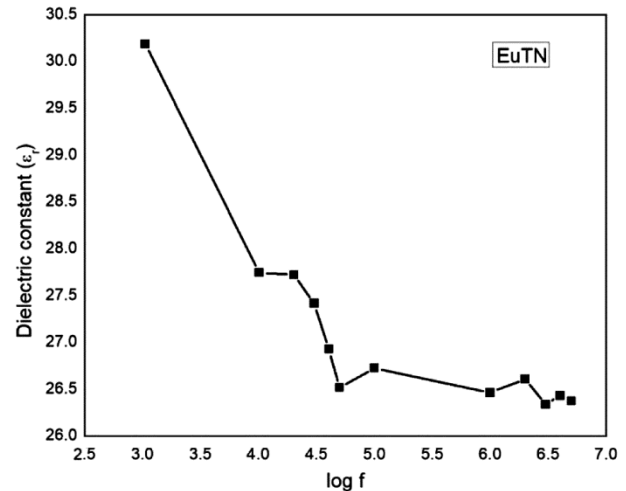


Fig. 8 — The variation of dielectric constant with frequency

constant and the loss factor decrease on increasing frequency at room temperature (Fig. 8 and Fig. 9). The decrease in the dielectric constant arises from the lack of spontaneous polarization in the dielectric material with the application of electric field due to the inertia possessed by the charge. This theory is known as Maxwell-Wagner interfacial polarization<sup>14</sup>. Dielectric constant reaches a stable value of nearly 26.5 for the sample EuTN at higher frequency side. In addition, it is also observed that the dielectric constant and loss factor became independent of frequency at higher frequency region. The observed variations in  $\tan \delta$  with frequency are explained by space charge polarization using Koop's theory<sup>15</sup>.

In accordance with the universal power law, the variation of ac conductivity with the radio frequency shows a frequency independent plateau in the low frequency region as in Fig. 10. The variation from the plateau region in the ac conductance at high

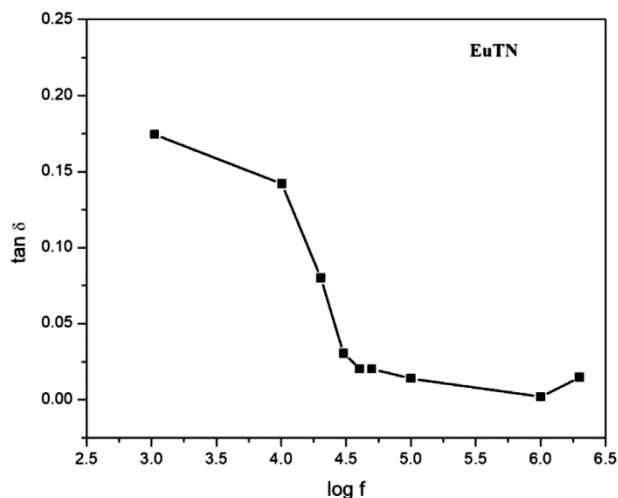


Fig. 9 — The variation of loss factor with frequency

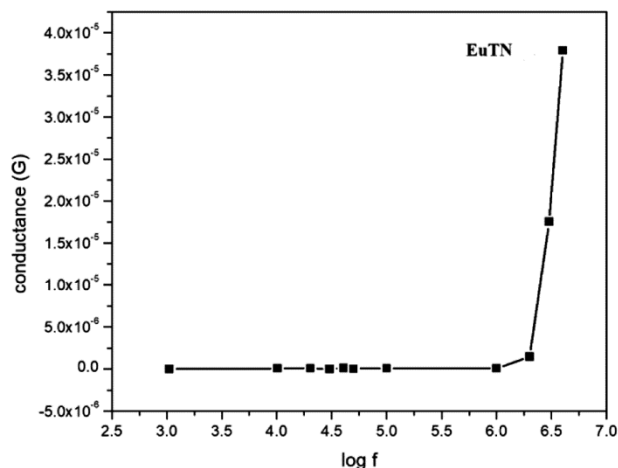


Fig. 10 — The variation of conductance with frequency

frequency is due to the electrode polarization effect in the dielectric material. The value of permittivity and the low dielectric loss makes the ceramic suitable for resonator applications in radio frequency communication systems.

## 5 Conclusions

The nanostructured dielectric ceramic  $\text{EuTiNbO}_6$ , was synthesized through auto ignited combustion technique. The X-ray diffraction pattern shows that the sample is single phase and crystallizes in orthorhombic aeschynite structure. The vibrational spectroscopic studies confirmed the XRD results.

The crystallite size obtained from Scherrer's formula is in good agreement with TEM results. The surface morphology of the sintered sample was analyzed using SEM. The constituent elements of the sample were distinguished by analyzing the EDS spectrum. The dielectric constant and quality factor at microwave frequency region were estimated as 35 and 23370, respectively which indicate that the material is suitable for microwave applications. The variation of dielectric properties in radio frequency region has been explained in the light of Maxwell-Wagner interfacial polarization, Universal power law and Koops phenomenological theory of dielectrics. The enhanced dielectric properties in both radio and microwave frequency range of  $\text{EuTiNbO}_6$  nanoparticles may be due to the quantum confinement property of Nano particles. The radio and microwave frequency studies show that the material can effectively be used as dielectric resonators in communication circuits due to its high value of dielectric constant and low dielectric loss.

## References

- 1 Komkov I, *Dokl Acad Nauk SSSR*, 148 (1963) 1182.
- 2 Sebastian M T, Solomon S & Ratheesh R, *J Am Ceram Soc*, 84 (2001) 1487.
- 3 Solomon S, Joseph J T, Kumar H P & Thomas J K, *J Mater Lett*, 60 (2006) 2814.
- 4 Jacob L, Padmakumar H, Gopchandran K G, Thomas J K & Solomon S, *J Mater Sci Mater Electron*, 18 (2007) 8.
- 5 Kumar H P, Thomas J K, Varma M R & Solomon S, *J Alloy Compd*, 455 (2008) 475.
- 6 Fergy J, Annamma J, Jijimon K T & Sam S, *J Mater Sci Mater Electr*, 28 (2017) 5997.
- 7 Fergy J, Jijimon K T, John J & Sam S, *J Elect Mater*, 28 (2017) 5536.
- 8 Fergy J, John J, Jijimon K T & Sam S, *J Asian Ceram Soc*, 271 (2017) 1016.
- 9 Tyagi A K, Chavanand S V & Purohit R D, *Indian J Pure Appl Phys*, 44 (2006) 113.
- 10 Tyagi A K & Purohit R D, *IANCAS Bull*, 6 (2007) 120.
- 11 Patil K C, Aruna S T & Mimani T, *Curr Opin Sol State Mater Sci*, 6 (2002) 507.
- 12 Nakamoto K, *Infrared and Raman Spectra of Inorganic and Coordination Compounds*, Wiley, New York, (1986).
- 13 Gleiter H, *Acta Mater*, 481 (2000) 29.
- 14 Maxwell J C, *A treatise on Electricity and Magnetism*, Oxford University Press, Oxford, (1954).
- 15 Koops C G, *Phys Rev*, 83 (1951) 121.